Supplement of Adv. Stat. Clim. Meteorol. Oceanogr., 6, 223–244, 2020
https://doi.org/10.5194/ascmo-6-223-2020-supplement

ASCMO
Open Access

Supplement of

A machine learning approach to emulation and biophysical parameter estimation with the Community Land Model, version 5

Katherine Dagon et al.

Correspondence to: Katherine Dagon (kdagon@ucar.edu)

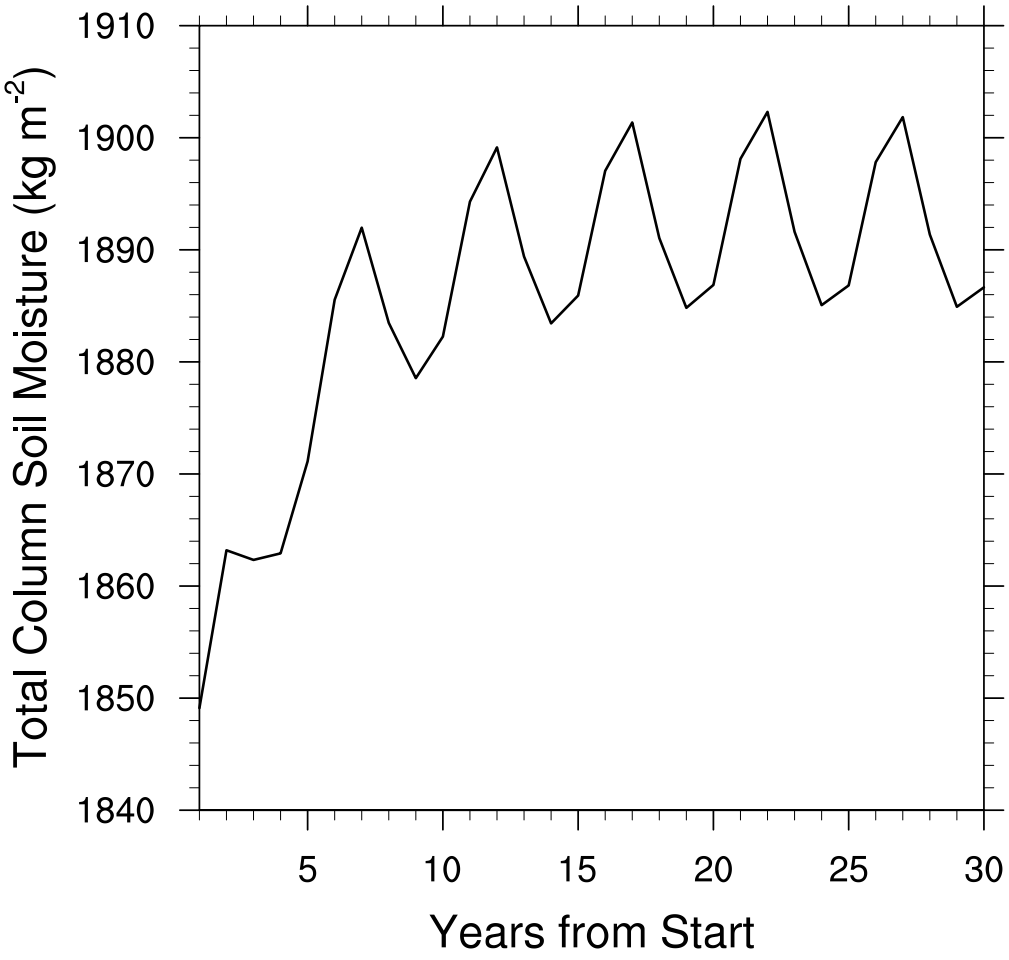

Figure S1: Global, annual mean total column soil moisture (kg m^{-2}) over a 30 year simulation period with default CLM5 parameter values. After 15 years the soil moisture has reach equilibrium.

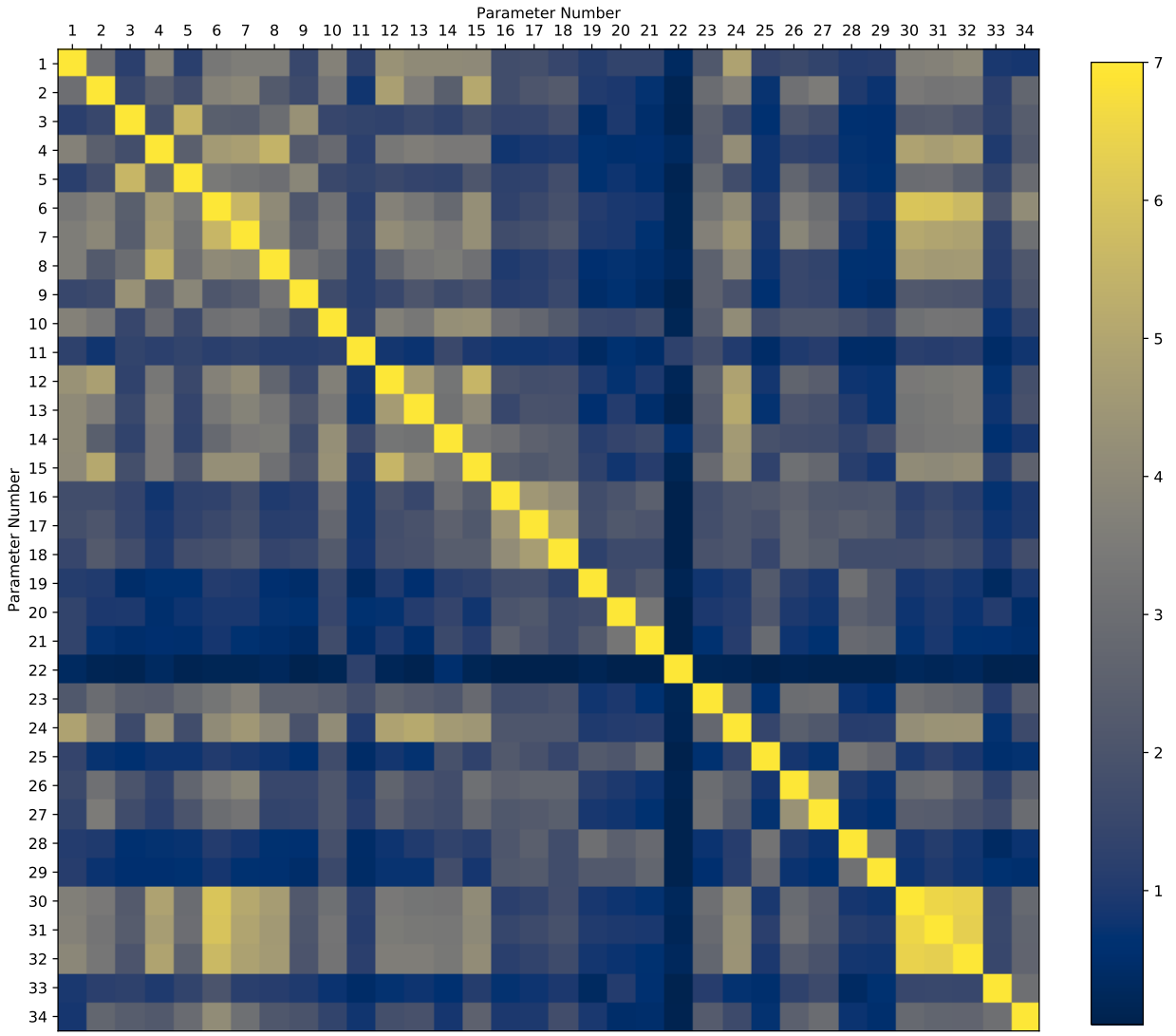

Figure S2: Heatmap showing the spatial pattern correlations between each pairwise parameter combination. The pattern correlations are summed across the seven output variables, such that a perfect correlation is 7 (as seen along the diagonal showing the correlations of each parameter with itself). Parameter numbering follows Table S1.

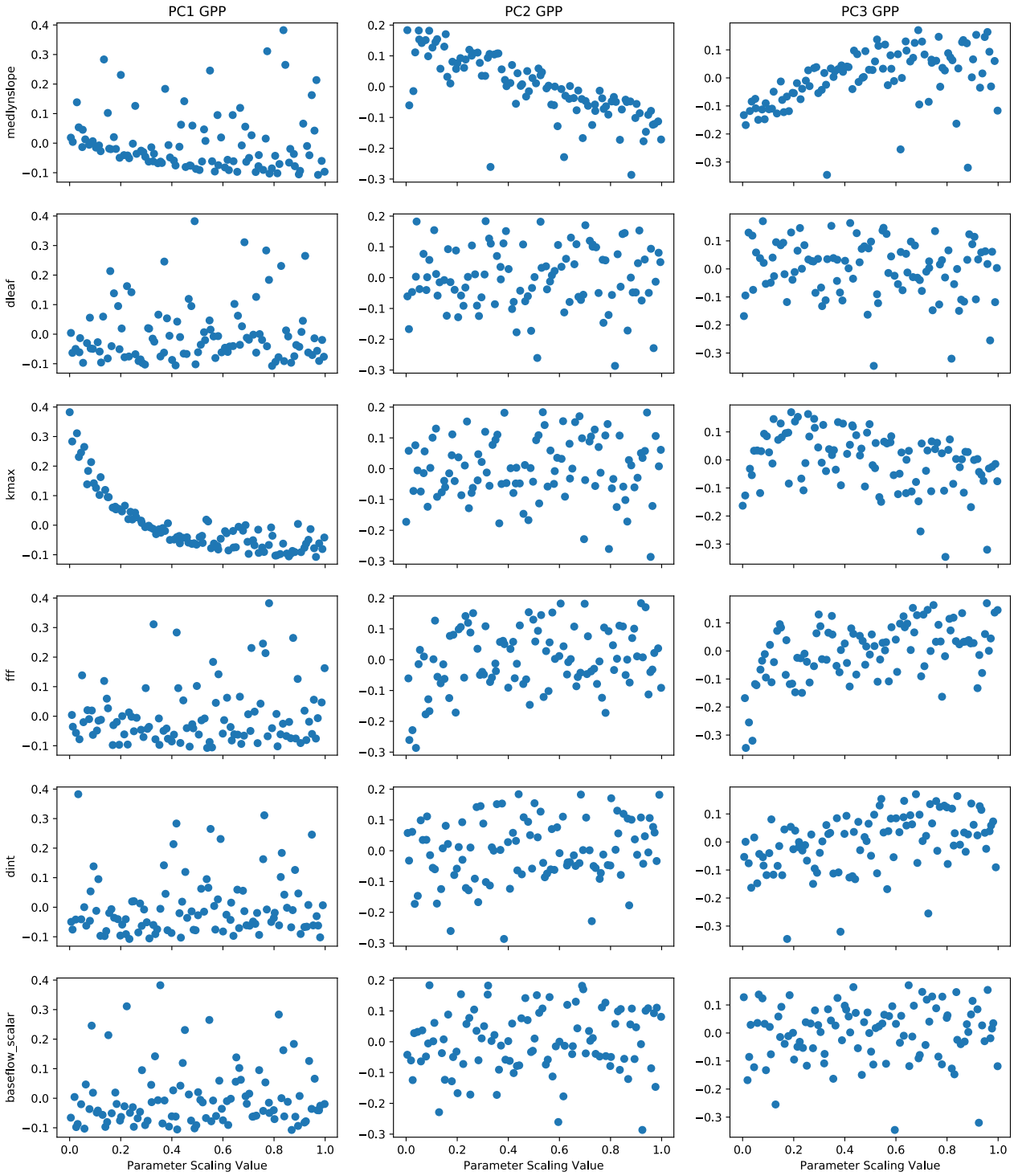

Figure S3: Scatterplot of PC1 (left column), PC2 (center column), and PC3 (right column) for GPP from the CLM PPE, versus parameter scaling values. The y-axis of each panel shows the PC values, and each row represents a different parameter as indicated in the y-axis labels.

Figure S4: As in Figure S3, for LHF.

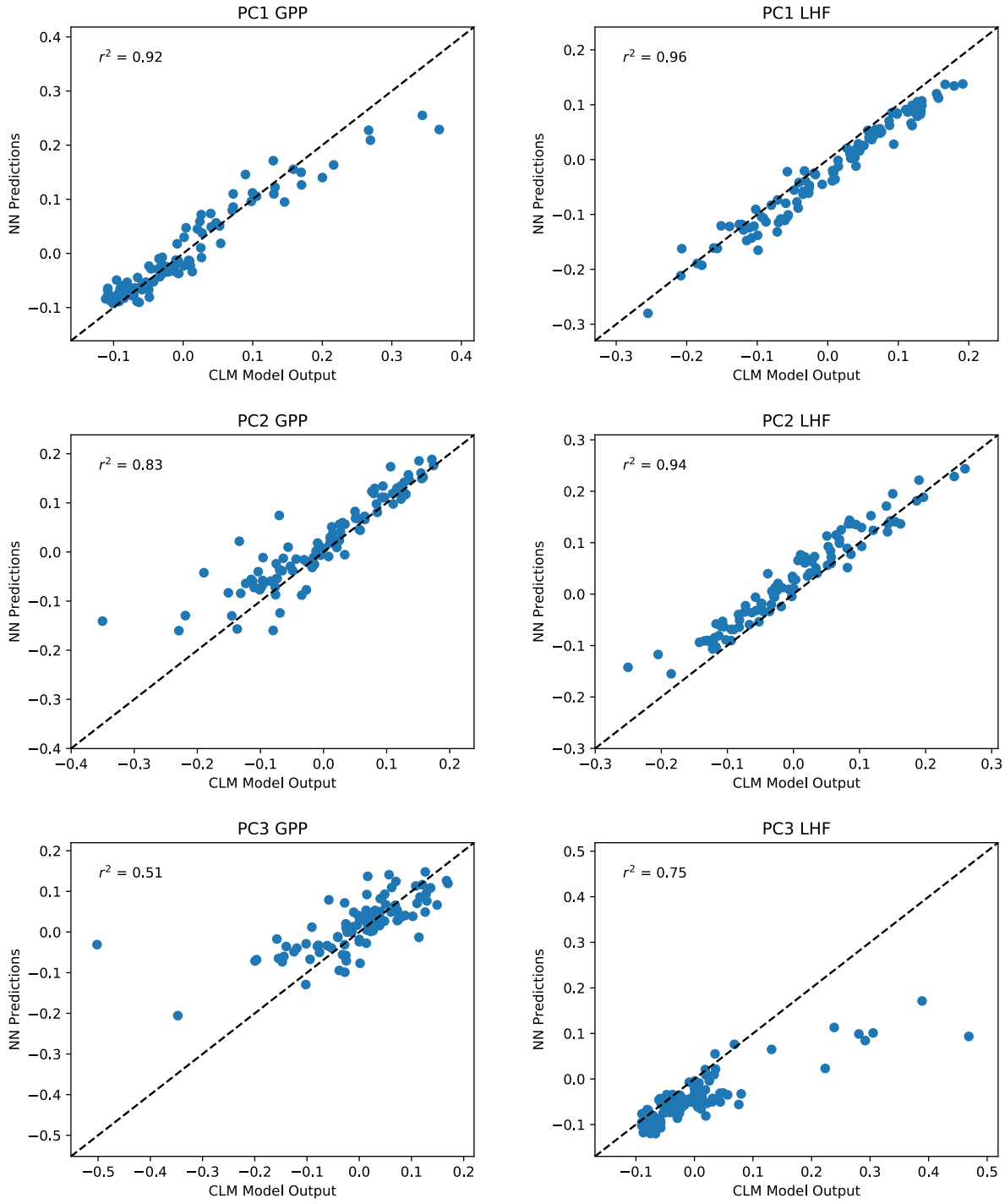

Figure S5: Scatterplot of predicted PC1, PC2, and PC3 for GPP (left column) and LHF (right column) from the neural network emulators, versus actual values from the second CLM PPE, representing a large out-of-sample validation test. The one-to-one line is shown on each panel as a dashed black line, and r^2 values from a linear regression fit are included in each panel in the upper left corner.

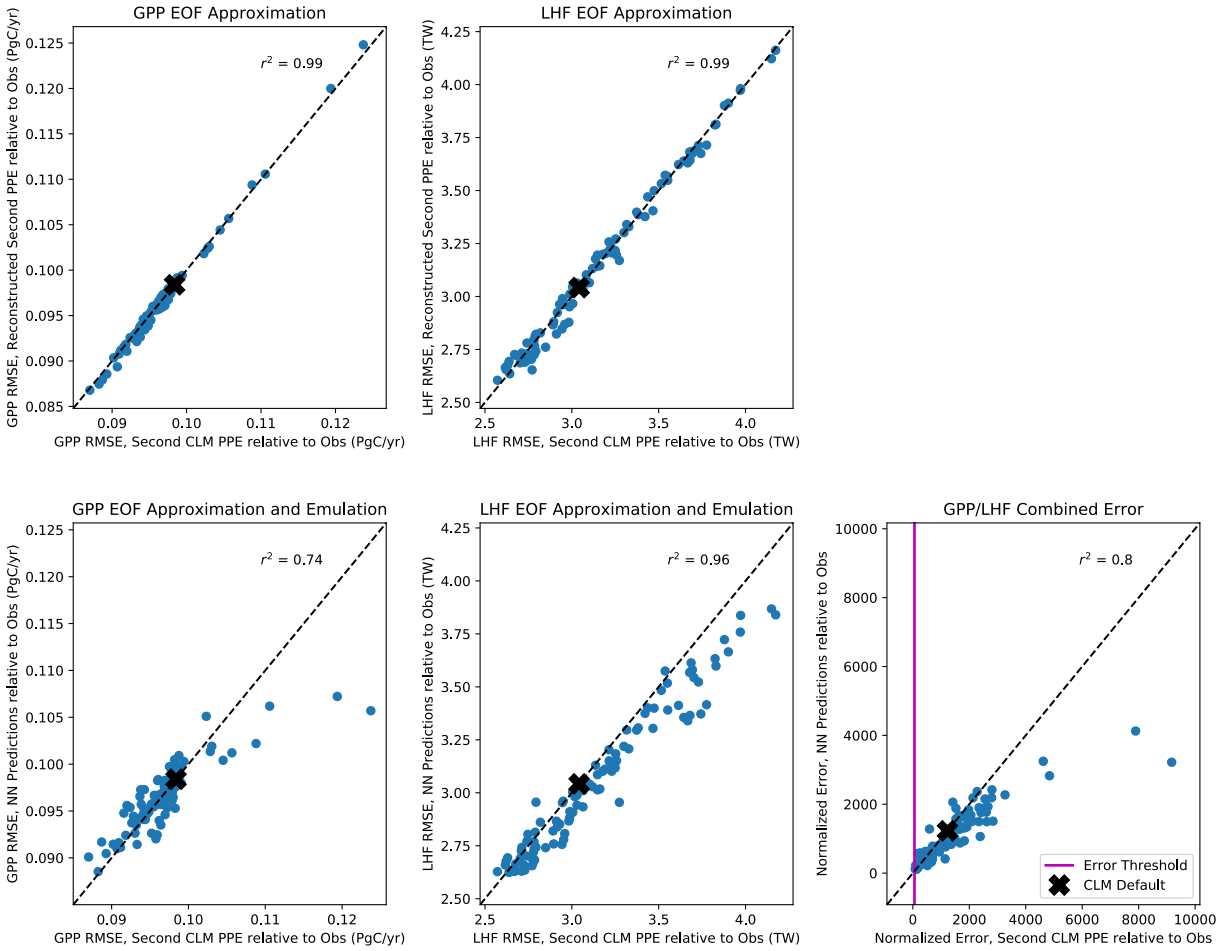

Figure S6: Scatterplot of root mean squared error (RMSE) across spatial gridpoints for GPP (first column) and LHF (second column) from the reconstructed EOF approximation relative to observations (top row), and the reconstructed neural network (NN) predictions relative to observations (bottom row) versus RMSE from the second CLM PPE relative to observations. The fifth panel in the bottom right shows the combined GPP/LHF normalized error relative to observations, for the NN predictions versus the second CLM PPE. The error threshold for the history matching experiment shown as a vertical magenta line. The default model errors are shown as a black x on each panel. The one-to-one line is shown on each panel as a dashed black line, and r^2 values from a linear regression fit are included at the top of each panel.

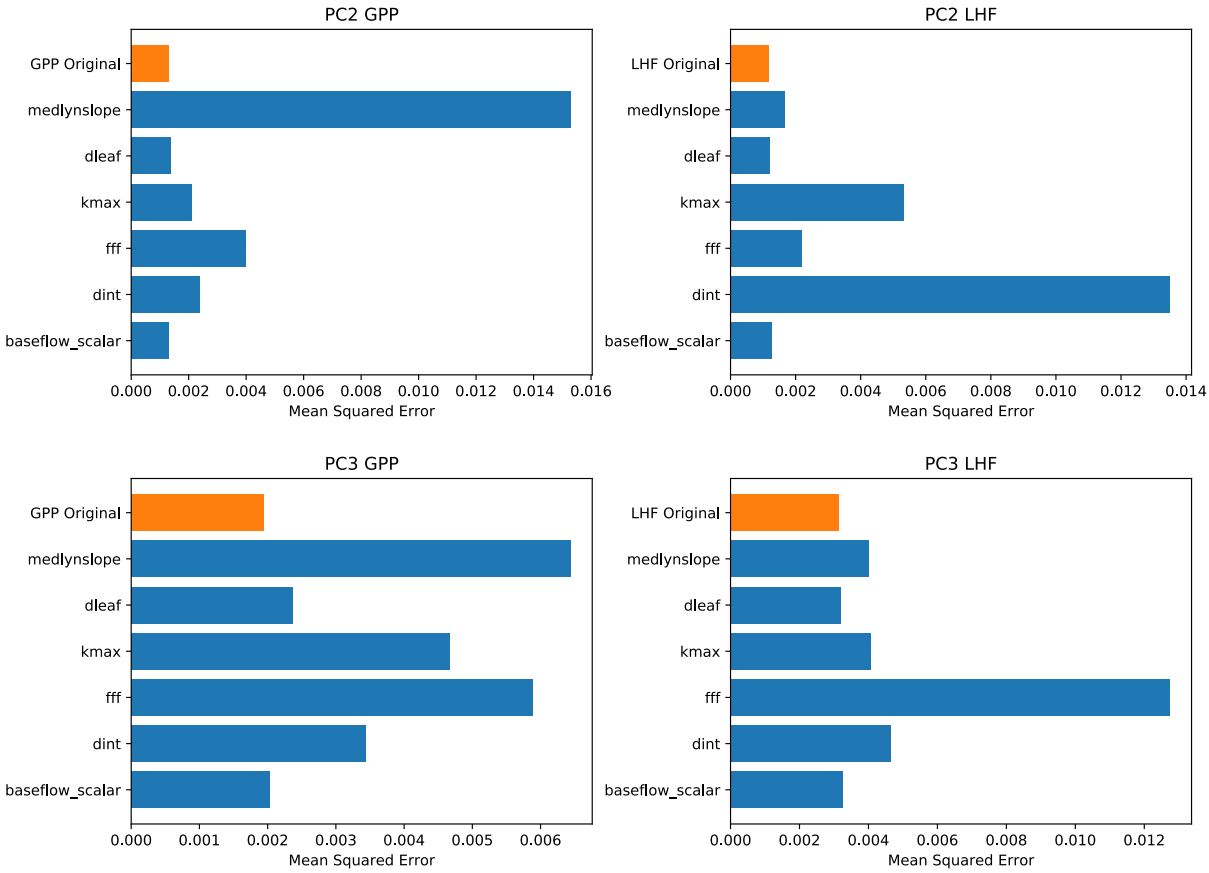

Figure S7: Permutation feature importance test of PC2 and PC3 for GPP (left column) and LHF (right column) from the neural network emulators. The top bar (in orange) shows the mean squared error without any permutation (original model skill), and each row (in blue) shows the emulator performance when the information from each parameter is removed, one at a time.

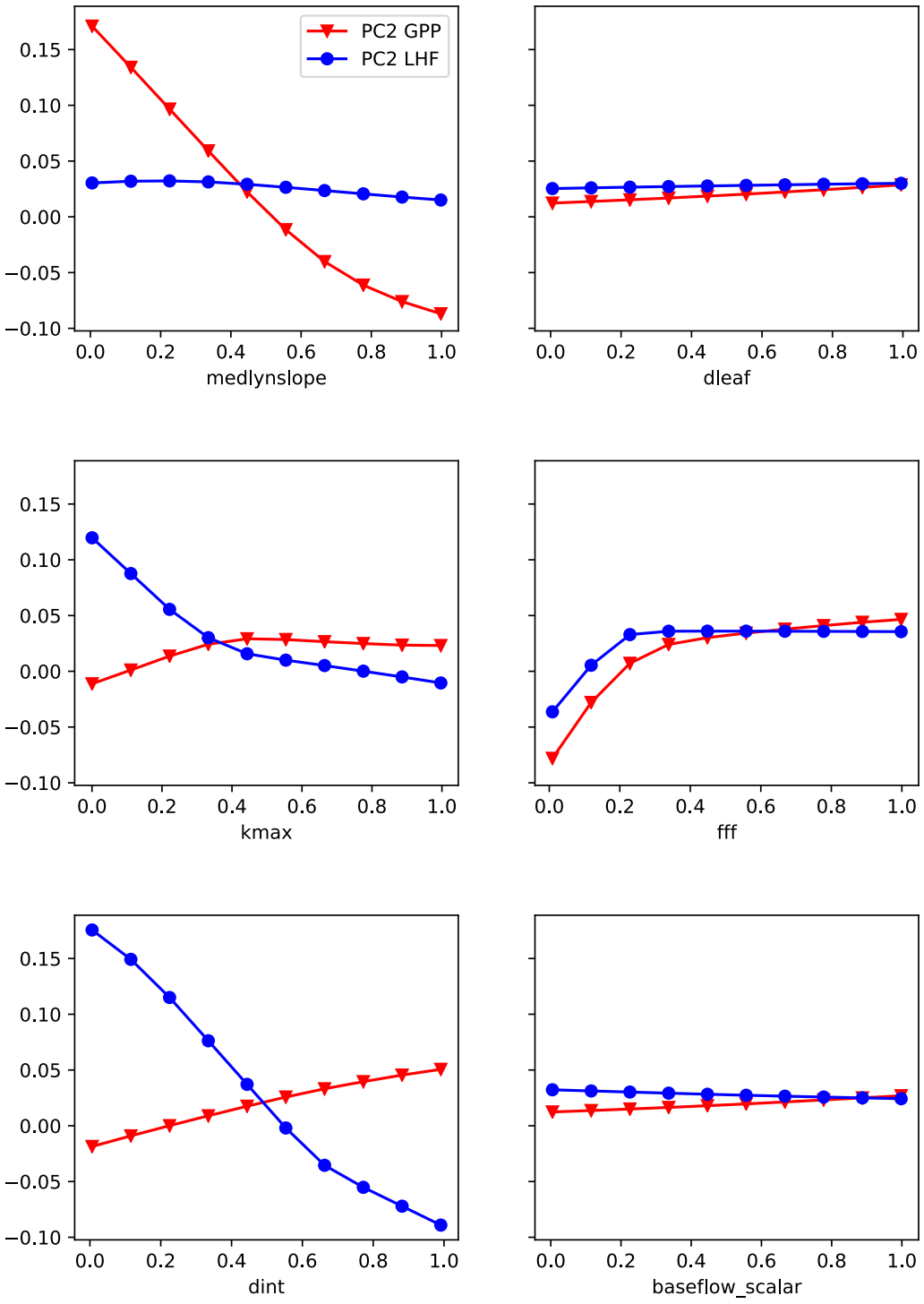

Figure S8: Partial dependence plots of PC2 for GPP (red) and LHF (blue) from the neural network emulators. Circles and triangles denote the fixed values used for predictions with each parameter. The x-axis shows the parameter scaling values, and the y-axis shows the average predictions of PC2.

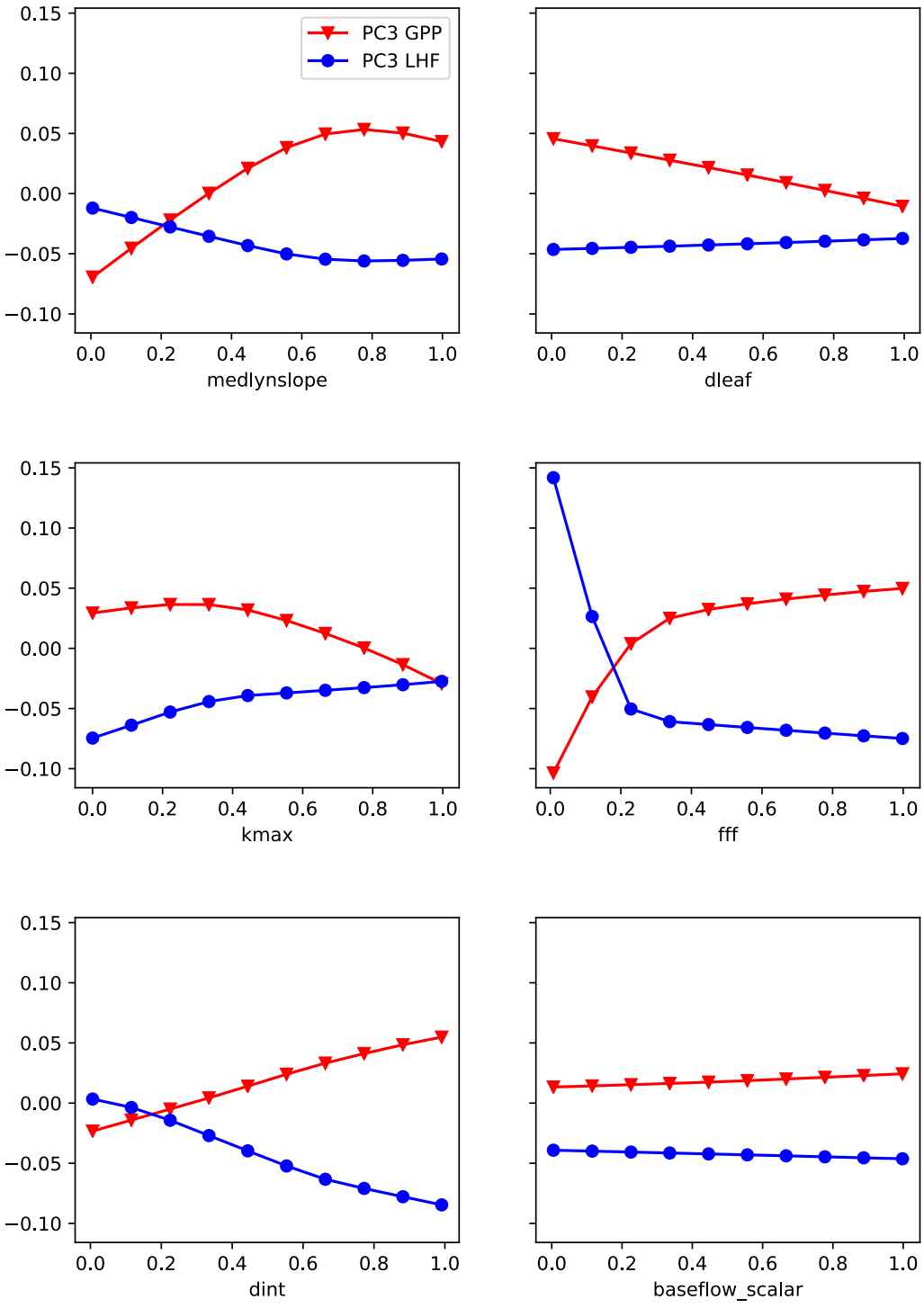

Figure S9: As in Figure S8, for PC3 of GPP and LHF.

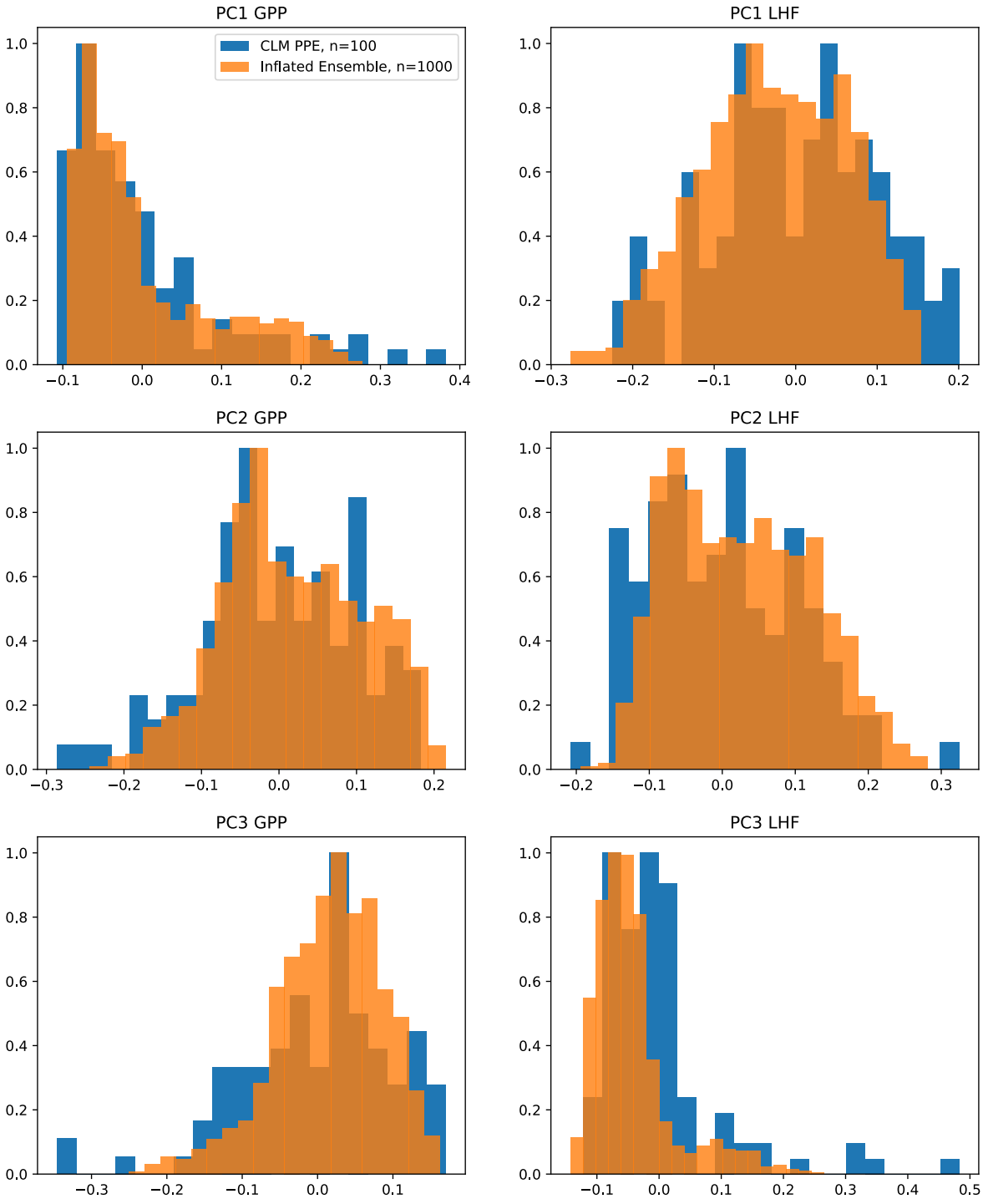

Figure S10: Normalized distributions of PC1, PC2, and PC3 for GPP (left column) and LHF (right column) comparing the neural network predictions for the inflated ensemble in orange (n=1000) with the original CLM PPE results in blue (n=100).

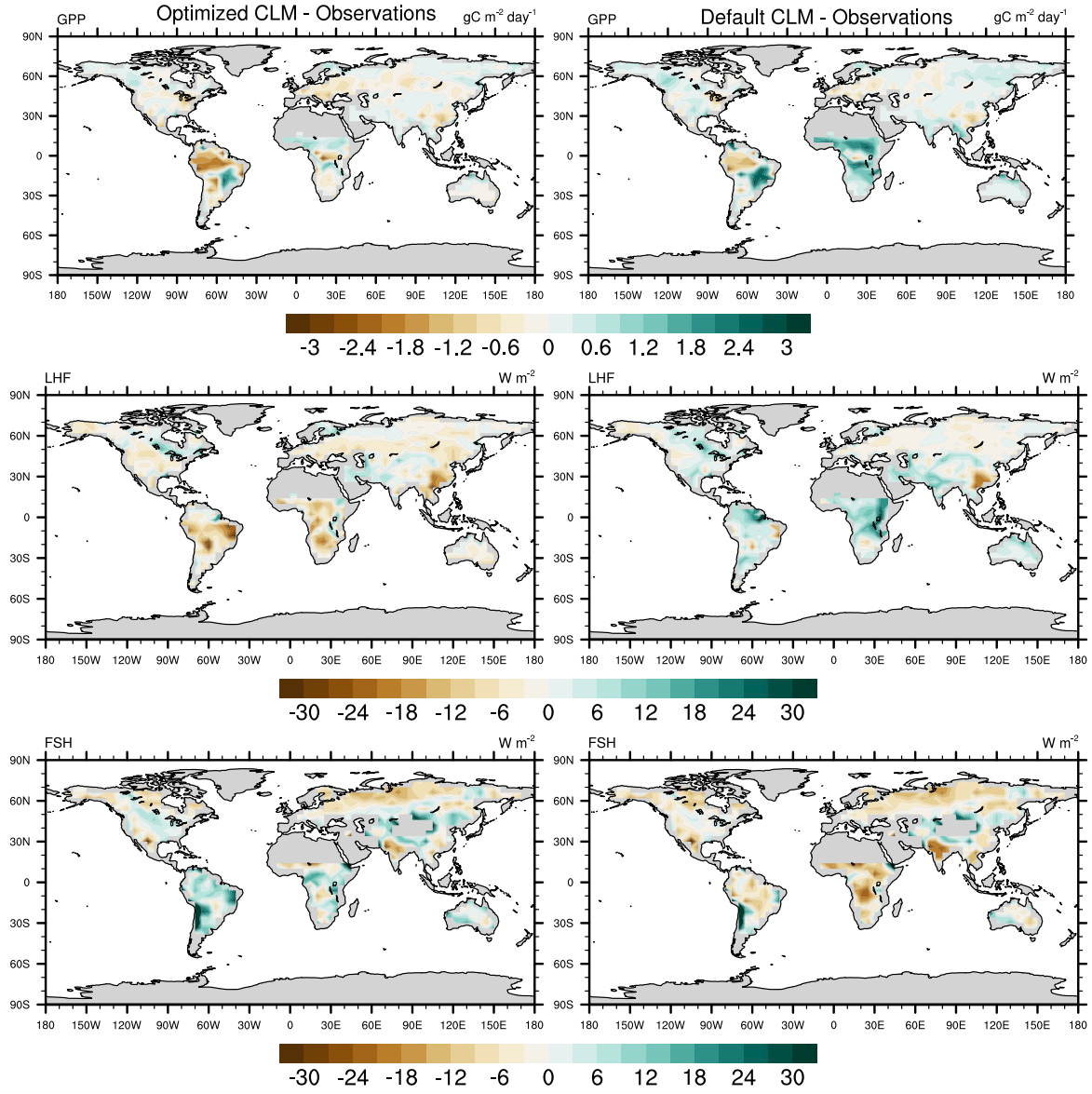

Figure S11: Annual mean bias maps comparing CLM with optimized parameters (left column) and the default CLM configuration (right column) with observations. The differences are calculated for the calibrated output variables (GPP and LHF), along with sensible heat flux (FSH), an additional model output that we did not calibrate to. The optimization approach shown here used an alternate cost function formulation to the approach shown in Eq. (6) by removing the weighting by modes of variability. The optimization results (parameter values and CLM test simulation) are nearly unchanged with this alternate formulation.

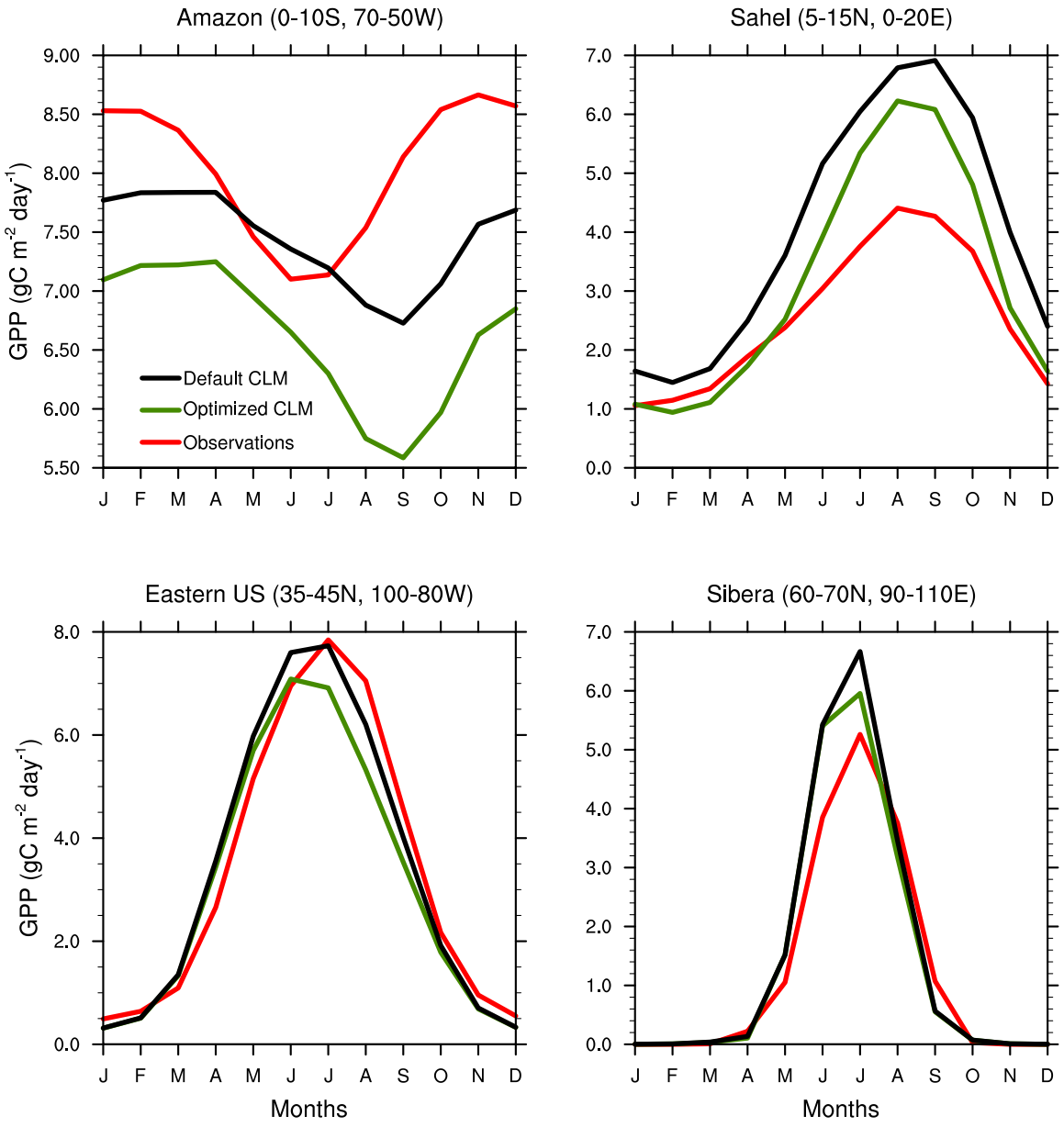

Figure S12: Monthly climatology of GPP across four different regions, comparing CLM with default parameters (black lines), CLM with optimized parameters (green lines), and observations (red lines).

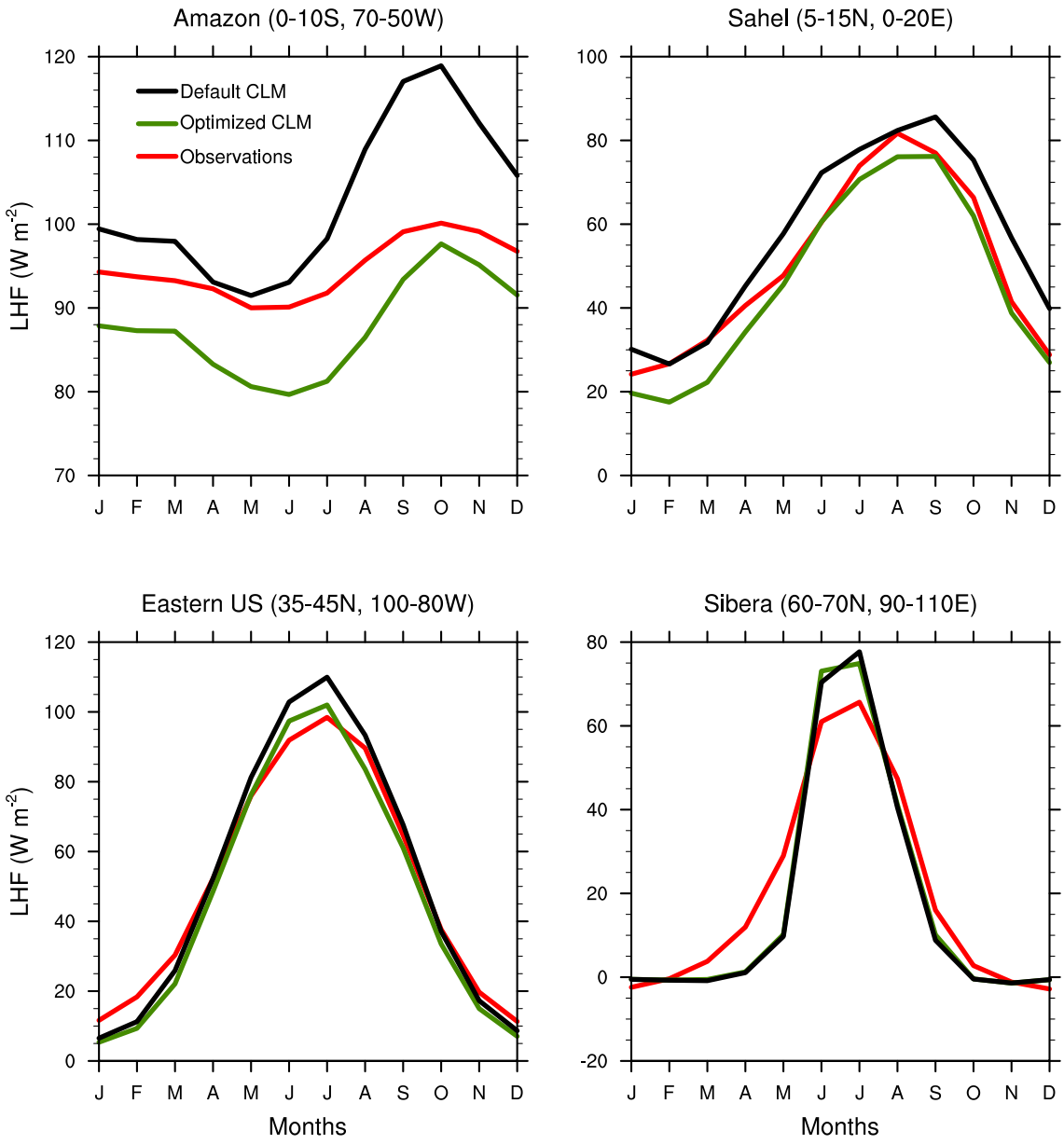

Figure S13: As in Figure S12, for LHF.

Table S1: Names and descriptions for 34 CLM5 biophysical parameters studied in the sensitivity analysis. The last column denotes whether or not the parameter varies with plant functional type (PFT).

	Parameter Name	Description (Units)	Varies with PFT?
1	displar	Ratio of displacement height to canopy top height	Yes
2	dleaf	Characteristic dimension of leaves in the direction of wind flow (m)	Yes
3	froot_leaf	New fine root carbon per new leaf carbon (gC gC^{-1})	Yes
4	kmax	Plant segment maximum conductance (s^{-1})	Yes
5	krmax	Root segment maximum conductance (s^{-1})	Yes
6	leafcn	Leaf carbon to nitrogen ratio (gC gN^{-1})	Yes
7	medlynslope	Slope of stomatal conductance-photosynthesis relationship (μmol H_2O μmol CO_2^{-1})	Yes
8	psi50	Water potential at 50% loss of conductance (mm H_2O)	Yes
9	rootprof_beta	Rooting beta parameter for carbon and nitrogen vertical discretization	Yes
10	z0mr	Ratio of momentum roughness length to canopy top height	Yes
11	baseflow_scalar	Scalar multiplier for base flow rate	No
12	maximum_leaf_wetted_fraction	Maximum fraction of leaf that may be wet prior to drip occurring	No
13	interception_fraction	Fraction of intercepted precipitation	No
14	csoilc	Drag coefficient for soil under dense canopy	No
15	cv	Turbulent transfer coefficient between canopy surface and canopy air (m $s^{-1/2}$)	No
16	a	Drag coefficient under less dense canopy	No
17	a2	Drag exponent under less dense canopy	No
18	zlnd	Momentum roughness length for soils, glacier, and wetland (m)	No
19	zsno	Momentum roughness length for snow (m)	No
20	laidl	Plant litter area index (m^2 m^{-2})	No
21	zdl	Litter layer thickness (m)	No
22	sy	Minimum specific yield	No
23	fff	Decay factor for fractional saturated area (m^{-1})	No
24	dewmx	Maximum storage of liquid water on leaf surface (kg m^{-2})	No
25	psno	Maximum storage of snow on leaf surface (kg m^{-2})	No
26	dmax	Dry surface layer (DSL) parameter (mm)	No
27	dint	Fraction of saturated soil for moisture value at which DSL initiates	No
28	kaccum	Accumulation constant for fractional snow covered area	No
29	nmelt	Parameter controlling shape of snow-covered area	No
30	kc25	Michaelis-Menten constant at 25^{o}C for CO_2 (μmol mol^{-1})	No
31	ko25	Michaelis-Menten constant at 25^{o}C for O_2 (mmol mol^{-1})	No
32	cp25	CO_2 compensation point at 25^{o}C (μmol mol^{-1})	No
33	fnr	Mass ratio of total Rubisco molecular mass to nitrogen in Rubisco (gRubisco gN(Rubisco)$^{-1}$)	No
34	act25	Specific activity of Rubisco at 25^{o}C (μmol CO_2 $gRubisco^{-1}$ s^{-1})	No

Table S2: Sensitivity ranges for the CLM5 biophysical parameters listed in Table S1. For some PFT-varying parameters, the default values are shown as a list or a range, and the minimum and maximum values are shown relative to the default value.

Parameter Name	Default Value(s)	Minimum	Maximum	Reference(s)
displar	0.67, 0.68	0.4	0.95	[68, 45, 53]
dleaf	0.04	See Table S6		[26, 44, 6, 42]
froot_leaf	1, 1.5, 2	default × 0.8	default × 1.2	[1, 31, 21, 38, 34]
kmax	2×10^{-8}	2×10^{-9}	3.8×10^{-8}	[28, 4, 8, 55, 56, 63]
krmax	1×10^{-11}–1.995×10^{-8}	default × 0.1	default × 1.9	[28, 4, 8, 55, 56, 63]
leafcn	20–58	default × 0.69	default × 1.44	[62, 60]
medlynslope	1.62–9	See Table S7		[30, 37, 32, 10]
psi50	-5.3×10^{5}– -1.5×10^{5}	default × 0.9	default × 1.1	[28, 33]
rootprof_beta	0.914–0.993	default × 0.995	default × 1.005	[22]
z0mr	0.055, 0.075, 0.12	default × 0.6	default × 1.5	[68, 45, 53]
baseflow_scalar	1×10^{-3}	5×10^{-4}	0.1	*Author estimates*
maximum_leaf_wetted_fraction	0.05	0.01	0.5	*Author estimates*
interception_fraction	1	0.5	1	*Author estimates*
csoilc	4×10^{-3}	2.5×10^{-3}	1.2×10^{-2}	[13, 66, 49]
cv	1×10^{-2}	5×10^{-3}	2×10^{-2}	[11, 13, 66]
a	0.13	0.1	0.13	[67, 66]
a2	0.45	0.45	0.5	[67, 66]
zlnd	1×10^{-2}	3×10^{-3}	5×10^{-2}	[67, 25]
zsno	2.4×10^{-3}	1×10^{-5}	7×10^{-2}	[7, 35, 18]
laidl	0.5	0.5	1.5	[49]
zdl	0.05	0.01	0.1	[50, 49]
sy	0.02	0.01	0.02	[40]
fff	0.5	0.02	5	[39, 20, 16, 15]
dewmx	0.1	0.05	2	[46, 48, 47, 11, 36, 12, 41, 13, 27]
psno	6	1.4	9.5	[43, 19, 57]
dmax	15	10	60	[59, 61, 17, 54]
dint	0.8	0.5	1	[59]
kaccum	0.1	0.1	0.4	[58]
nmelt	200	180	220	[58]
kc25	404.9	266	454	[2, 23, 65, 24, 64, 9, 52, 3]
ko25	278.4	207	395	[2, 23, 65, 24, 64, 9, 52, 3]
cp25	42.75	35	44.7	[3, 5]
fnr	7.16	7.14	7.16	[29, 62, 60]
act25	60	40	120	[14, 51, 64, 60]

Table S3: Parameter effect (PE) ranks for seven different outputs of interest: Gross Primary Production (GPP), Evapotranspiration (ET), Transpiration Fraction (TF), Sensible Heat Flux (SHF), 10 cm Soil Moisture (SM10), Total Column Soil Moisture (SMTOT) and Water Table Depth (WTD).

Parameter Name	GPP	ET	TF	SHF	SM10	SMTOT	WTD	Average Value of PE Ranks Across Outputs	Overall PE Rank
medlynslope	4	1	1	1	2	2	3	2	1
kmax	1	2	3	2	5	5	4	3.14	2
fff	5	4	5	4	1	1	2	3.14	2
dint	9	3	6	3	4	3	5	4.71	4
dmax	12	5	4	5	3	4	6	5.57	5
leafcn	2	7	7	7	6	7	7	6.14	6
maximum_leaf_wetted_fraction	13	6	2	6	8	9	8	7.43	7
krmax	6	10	14	11	7	8	9	9.29	8
cv	11	9	9	9	10	12	10	10	9
dleaf	14	8	13	8	9	10	11	10.43	10
act25	3	11	18	13	13	11	12	11.57	11
kc25	7	12	15	14	12	13	13	12.29	12
ko25	8	15	10	17	16	15	15	13.71	13
dewmx	17	13	12	16	19	18	14	15.57	14
zsno	23	18	16	10	11	16	16	15.71	15
z0mr	19	14	20	15	17	22	17	17.71	16
baseflow_scalar	22	23	32	27	14	6	1	17.86	17
zlnd	20	17	22	12	18	19	22	18.57	18
psi50	15	20	17	22	22	17	20	19	19
cp25	10	19	25	20	21	20	18	19	19
rootprof_beta	16	21	31	25	20	14	19	20.86	21
interception_fraction	21	16	28	18	25	23	21	21.71	22
csoilc	24	22	19	23	27	25	23	23.29	23
froot_leaf	18	24	26	28	23	21	24	23.43	24
kaccum	29	28	21	24	15	24	26	23.86	25
displar	25	25	8	26	29	28	28	24.14	26
a	26	26	23	21	24	26	27	24.71	27
a2	27	27	27	19	26	27	25	25.43	28
psno	28	30	11	29	30	30	31	27	29
nmelt	31	29	29	30	28	29	29	29.29	30
zdl	32	31	24	31	31	31	30	30	31
laidl	33	32	30	32	32	32	32	31.86	32
fnr	30	33	33	33	33	33	33	32.57	33
sy	34	34	34	34	34	34	34	34	34

Table S4: Spatial pattern correlations and ranks summed across seven different outputs (as shown in Fig. S2) and averaged across each parameter combination.

Parameter Name	Average Pattern Correlation	Pattern Correlation Rank
sy	0.389	1
baseflow_scalar	1.169	2
fnr	1.189	3
zsno	1.306	4
nmelt	1.350	5
laidl	1.368	6
zdl	1.369	7
psno	1.438	8
kaccum	1.452	9
rootprof_beta	1.836	10
froot_leaf	1.930	11
act25	1.974	12
a	1.990	13
a2	2.020	14
zlnd	2.038	15
dint	2.057	16
krmax	2.114	17
dmax	2.244	18
fff	2.267	19
csoilc	2.490	20
displar	2.51987	21
interception_fraction	2.51991	22
dleaf	2.528	23
kmax	2.532	24
psi50	2.534	25
z0mr	2.593	26
maximum_leaf_wetted_fraction	2.624	27
dewmx	2.864	28
cp25	2.887	29
cv	2.890	30
kc25	2.933	31
ko25	2.963	32
medlynslope	3.016	33
leafcn	3.037	34

Table S5: Parameter Effect (PE) ranks and Pattern Correlation (PC) ranks, along with the average and overall ranks across these metrics.

Parameter Name	PE Rank	PC Rank	Average Rank	Overall Rank
baseflow_scalar	17	2	9.5	1
zsno	15	4	9.5	1
dint	4	16	10	3
fff	2	19	10.5	4
act25	11	12	11.5	5
dmax	5	18	11.5	5
krmax	8	17	12.5	7
kmax	2	24	13	8
rootprof_beta	21	10	15.5	9
zlnd	18	15	16.5	10
dleaf	10	23	16.5	10
kaccum	25	9	17	12
maximum_leaf_wetted_fraction	7	27	17	12
medlynslope	1	33	17	12
sy	34	1	17.5	15
nmelt	30	5	17.5	15
froot_leaf	24	11	17.5	15
fnr	33	3	18	18
psno	29	8	18.5	19
laidl	32	6	19	20
zdl	31	7	19	20
cv	9	30	19.5	22
a	27	13	20	23
leafcn	6	34	20	23
a2	28	14	21	25
z0mr	16	26	21	25
dewmx	14	28	21	25
csoilc	23	20	21.5	28
kc25	12	31	21.5	28
interception_fraction	22	22	22	30
psi50	19	25	22	30
ko25	13	32	22.5	32
displar	26	21	23.5	33
cp25	19	29	24	34

Table S6: Plant functional type (PFT) specific sensitivity ranges for dleaf, the characteristic dimension of leaves in the direction of wind flow. The leaf width and PFT identifying data is from [44] and the calculation of dleaf from leaf width is based on the equations of [6]. Due to lack of data, Crop PFTs use the minimum and maximum leaf width values from grasses and shrubs combined.

PFT Name	Minimum observed leaf width (cm)	Maximum observed leaf width (cm)	Assumed leaf shape	Minimum dleaf (m)	Maximum dleaf (m)
Needleleaf Evergreen Temperate Tree	0.03	0.15	Needle	2.16×10^{-4}	1.08×10^{-3}
Needleleaf Evergreen Boreal Tree	0.03	0.15	Needle	2.16×10^{-4}	1.08×10^{-3}
Needleleaf Deciduous Boreal Tree	0.1	0.5	Needle	7.2×10^{-4}	3.6×10^{-3}
Broadleaf Evergreen Tropical Tree	1	7	Circular	8.1×10^{-3}	5.67×10^{-2}
Broadleaf Evergreen Temperate Tree	1	7	Circular	8.1×10^{-3}	5.67×10^{-2}
Broadleaf Deciduous Tropical Tree	1	30	Circular	8.1×10^{-3}	0.243
Broadleaf Deciduous Temperate Tree	1	30	Circular	8.1×10^{-3}	0.243
Broadleaf Deciduous Boreal Tree	1	30	Circular	8.1×10^{-3}	0.243
Broadleaf Evergreen Shrub	1	10	Circular	8.1×10^{-3}	8.1×10^{-2}
Broadleaf Deciduous Temperate Shrub	0.05	15	Circular	4.05×10^{-4}	0.1215
Broadleaf Deciduous Boreal Shrub	0.02	6	Circular	1.62×10^{-4}	4.86×10^{-2}
C3 Arctic Grass	0.02	2.5	Needle	1.44×10^{-4}	1.8×10^{-2}
C3 Non-Arctic Grass	0.02	2.5	Needle	1.44×10^{-4}	1.8×10^{-2}
C4 Grass	0.02	2.5	Needle	1.44×10^{-4}	1.8×10^{-2}
Crops	0.02	15	Circular	1.62×10^{-4}	0.1215

Table S7: Plant functional type (PFT) specific sensitivity ranges for medlynslope, the slope of stomatal conductance-photosynthesis relationship. The slope data is from [30]. Due to lack of data, C3 Arctic Grasses use a +/- 10% perturbation from the default value.

PFT Name	Minimum medlynslope (μmol H_2O μmol CO_2^{-1})	Maximum medlynslope (μmol H_2O μmol CO_2^{-1})
Needleleaf Evergreen Temperate Tree	1.29	4.70
Needleleaf Evergreen Boreal Tree	1.29	4.70
Needleleaf Deciduous Boreal Tree	1.29	4.70
Broadleaf Evergreen Tropical Tree	1.63	4.59
Broadleaf Evergreen Temperate Tree	1.63	4.59
Broadleaf Deciduous Tropical Tree	3.19	5.11
Broadleaf Deciduous Temperate Tree	3.19	5.11
Broadleaf Deciduous Boreal Tree	3.19	5.11
Broadleaf Evergreen Shrub	2.25	9.27
Broadleaf Deciduous Temperate Shrub	2.25	9.27
Broadleaf Deciduous Boreal Shrub	2.25	9.27
C3 Arctic Grass	2.00	2.44
C3 Non-Arctic Grass	3.05	9.45
C4 Grass	0.53	4.03
C3 Crop	3.46	7.70
C4 Crop	0.53	4.03

References

[1] O. K. Atkin, K. J. Bloomfield, P. B. Reich, M. G. Tjoelker, G. P. Asner, D. Bonal, G. Bönisch, M. G. Bradford, L. A. Cernusak, E. G. Cosio, et al. Global variability in leaf respiration in relation to climate, plant functional types and leaf traits. *New Phytologist*, 206(2):614–636, 2015.

[2] M. R. Badger and G. J. Collatz. Studies on the kinetic mechanism of ribulose-1, 5-bisphosphate carboxylase and oxygenase reactions, with particular reference to the effect of temperature on kinetic parameters. *Carnegie Institute of Washington Yearbook*, 76:355–361, 1977.

[3] C. J. Bernacchi, E. L. Singsaas, C. Pimentel, A. R. Portis Jr, and S. P. Long. Improved temperature response functions for models of rubisco-limited photosynthesis. *Plant, Cell & Environment*, 24(2):253–259, 2001.

[4] G. B. Bonan, M. Williams, R. A. Fisher, and K. W. Oleson. Modeling stomatal conductance in the earth system: linking leaf water-use efficiency and water transport along the soil-plant-atmosphere continuum. *Geoscientific Model Development*, 7(5):2193–2222, 2014.

[5] A. Brooks and G. D. Farquhar. Effect of temperature on the CO_2/O_2 specificity of ribulose-1, 5-bisphosphate carboxylase/oxygenase and the rate of respiration in the light. *Planta*, 165(3):397–406, 1985.

[6] G. S. Campbell and J. M. Norman. *Conductances for Heat and Mass Transfer*, pages 87–111. Springer New York, New York, NY, 1998.

[7] A. C. Chamberlain. Roughness length of sea, sand, and snow. *Boundary-Layer Meteorology*, 25(4):405–409, 1983.

[8] Y.-L. Chuang, R. Oren, A. L. Bertozzi, N. Phillips, and G. G. Katul. The porous media model for the hydraulic system of a conifer tree: linking sap flux data to transpiration rate. *Ecological Modelling*, 191(3-4):447–468, 2006.

[9] G. J. Collatz, J. T. Ball, C. Grivet, and J. A. Berry. Physiological and environmental regulation of stomatal conductance, photosynthesis and transpiration: a model that includes a laminar boundary layer. *Agricultural and Forest Meteorology*, 54(2-4):107–136, 1991.

[10] M. G. De Kauwe, J. Kala, Y.-S. Lin, A. J. Pitman, B. E. Medlyn, R. A. Duursma, G. Abramowitz, Y.-P. Wang, and D. G. Miralles. A test of an optimal stomatal conductance scheme within the CABLE land surface model. *Geoscientific Model Development*, 8(2):431–452, 2015.

[11] J. W. Deardorff. Efficient prediction of ground surface temperature and moisture, with inclusion of a layer of vegetation. *Journal of Geophysical Research: Oceans*, 83(C4):1889–1903, 1978.

[12] R. E. Dickinson. Modeling evapotranspiration for three-dimensional global climate models. *Climate Processes and Climate Sensitivity*, 29:58–72, 1984.

[13] R. E. Dickinson, A. Henderson-Sellers, and P. J. Kennedy. Biosphere-Atmosphere Transfer Scheme (BATS) Version 1e as Coupled to the NCAR Community Climate Model. Technical Report TN-387+STR, National Center for Atmospheric Research, 1993.

[14] J. R. Evans and J. R. Seemann. Differences between wheat genotypes in specific activity of ribulose-1, 5-bisphosphate carboxylase and the relationship to photosynthesis. *Plant Physiology*, 74(4):759–765, 1984.

[15] Y. Fan, H. Li, and G. Miguez-Macho. Global patterns of groundwater table depth. *Science*, 339(6122):940–943, 2013.

[16] Y. Fan and G. Miguez-Macho. A simple hydrologic framework for simulating wetlands in climate and earth system models. *Climate Dynamics*, 37(1-2):253–278, 2011.

[17] K.-U. Goss and M. Madliger. Estimation of water transport based on in situ measurements of relative humidity and temperature in a dry tanzanian soil. *Water Resources Research*, 43(5), 2007.

[18] C. Gromke, C. Manes, B. Walter, M. Lehning, and M. Guala. Aerodynamic roughness length of fresh snow. *Boundary-Layer Meteorology*, 141(1):21–34, 2011.

[19] N. R. Hedstrom and J. W. Pomeroy. Measurements and modelling of snow interception in the boreal forest. *Hydrological Processes*, 12(10-11):1611–1625, 1998.

[20] Z. Hou, M. Huang, L. R. Leung, G. Lin, and D. M. Ricciuto. Sensitivity of surface flux simulations to hydrologic parameters based on an uncertainty quantification framework applied to the community land model. *Journal of Geophysical Research: Atmospheres*, 117(D15), 2012.

[21] C. M. Iversen, V. L. Sloan, P. F. Sullivan, E. S. Euskirchen, A. D. McGuire, R. J. Norby, A. P. Walker, J. M. Warren, and S. D. Wullschleger. The unseen iceberg: plant roots in arctic tundra. *New Phytologist*, 205(1):34–58, 2015.

[22] R. B. Jackson, J. Canadell, J. R. Ehleringer, H. A. Mooney, O. E. Sala, and E. D. Schulze. A global analysis of root distributions for terrestrial biomes. *Oecologia*, 108(3):389–411, 1996.

[23] D. B. Jordan and W. L. Ogren. A sensitive assay procedure for simultaneous determination of ribulose-1, 5-bisphosphate carboxylase and oxygenase activities. *Plant Physiology*, 67(2):237–245, 1981.

[24] D. B. Jordan and W. L. Ogren. The CO_2/O_2 specificity of ribulose 1, 5-bisphosphate carboxylase/oxygenase. *Planta*, 161(4):308–313, 1984.

[25] A. B. Kara, A. Tribble, and P. H. Ruscher. Effects of roughness length on the FSU one-dimesional atmospheric boundary layer model forecast. *Atmósfera*, 11(4):239–256, 1998.

[26] J. Kattge, S. Díaz, S. Lavorel, I. C. Prentice, P. Leadley, G. Bönisch, E. Garnier, M. Westoby, P. B. Reich, I. J. Wright, J. H. C. Cornelissen, C. Violle, S. P. Harrison, P. M. v. Bodegom, M. Reichstein, B. J. Enquist, N. A. Soudzilovskaia, D. D. Ackerly, M. Anand, O. Atkin, M. Bahn, T. R. Baker, D. Baldocchi, R. Bekker, C. Blanco, B. Blonder, W. J. Bond, R. Bradstock, D. E. Bunker, F. Casanoves, J. Cavender-Bares, J. Q. Chambers, F. S. Chapin, J. Chave, D. Coomes, W. K. Cornwell, J. M. Craine, B. H. Dobrin, L. Duarte, W. Durka, J. Elser, G. Esser, M. Estiarte, W. F. Fagan, J. Fang, F. Fernández-Méndez, A. Fidelis, B. Finegan, O. Flores, H. Ford, D. Frank, G. T. Freschet, N. M. Fyllas, R. V. Gallagher, W. A. Green, A. G. Gutierrez, T. Hickler, S. Higgins, J. G. Hodgson, A. Jalili, S. Jansen, C. Joly, A. J. Kerkhoff, D. Kirkup, K. Kitajima, M. Kleyer, S. Klotz, J. M. H. Knops, K. Kramer, I. Kühn, H. Kurokawa, D. Laughlin, T. D. Lee, M. Leishman, F. Lens, T. Lenz, S. L. Lewis, J. Lloyd,

F. L. J. Llusià, S. Ma, M. D. Mahecha, P. Manning, T. Massad, B. Medlyn, J. Messier, A. T. Moles, S. C. Müller, K. Nadrowski, S. Naeem, U. Niinemets, S. Nöllert, A. Nüske, R. Ogaya, J. Oleksyn, V. G. Onipchenko, Y. Onoda, J. O. nez, G. Overbeck, W. A. Ozinga, S. P. no, S. Paula, J. G. Pausas, J. P. nuelas, O. L. Phillips, V. Pillar, H. Poorter, L. Poorter, P. Poschlod, A. Prinzing, R. Proulx, A. Rammig, S. Reinsch, B. Reu, L. Sack, B. Salgado-Negret, J. Sardans, S. Shiodera, B. Shipley, A. Siefert, E. Sosinski, J.-F. Soussana, E. Swaine, N. Swenson, K. Thompson, P. Thornton, M. Waldram, E. Weiher, M. White, S. White, S. J. Wright, B. Yguel, S. Zaehle, A. E. Zanne, and C. Wirth. TRY - a global database of plant traits. *Global Change Biology*, 17(9):2905–2935, 2011.

[27] R. F. Keim, A. E. Skaugset, and M. Weiler. Storage of water on vegetation under simulated rainfall of varying intensity. *Advances in Water Resources*, 29(7):974–986, 2006.

[28] D. Kennedy, S. C. Swenson, K. W. Oleson, D. M. Lawrence, R. Fisher, A. C. Lola da Costa, and P. Gentine. Implementing Plant Hydraulics in the Community Land Model, Version 5. *Journal of Advances in Modeling Earth Systems*, 11(2):485–513, 2019.

[29] G. D. Kuehn and B. A. McFadden. Ribulose-1, 5-diphosphate carboxylase from Hydrogenomonas eutropha and Hydrogenomonas facilis. II. Molecular weight, subunits, composition, and sulfhydryl groups. *Biochemistry*, 8(6):2403–2408, 1969.

[30] Y.-S. Lin, B. E. Medlyn, R. A. Duursma, I. C. Prentice, H. Wang, S. Baig, D. Eamus, V. R. de Dios, P. Mitchell, D. S. Ellsworth, M. O. de Beeck, G. Wallin, J. Uddling, L. Tarvainen, M.-L. Linderson, L. A. Cernusak, J. B. Nippert, T. W. Ocheltree, D. T. Tissue, N. K. Martin-StPaul, A. Rogers, J. M. Warren, P. De Angelis, K. Hikosaka, Q. Han, Y. Onoda, T. E. Gimeno, C. V. M. Barton, J. Bennie, D. Bonal, A. Bosc, M. Löw, C. Macinins-Ng, A. Rey, L. Rowland, S. A. Setterfield, S. Tausz-Posch, J. Zaragoza-Castells, M. S. J. Broadmeadow, J. E. Drake, M. Freeman, O. Ghannoum, L. B. Hutley, J. W. Kelly, K. Kikuzawa, P. Kolari, K. Koyama, J.-M. Limousin, P. Meir, A. C. Lola da Costa, T. N. Mikkelsen, N. Salinas, W. Sun, and L. Wingate. Optimal stomatal behaviour around the world. *Nature Climate Change*, 5(5):459–464, 2015.

[31] C. M. Litton, J. W. Raich, and M. G. Ryan. Carbon allocation in forest ecosystems. *Global Change Biology*, 13(10):2089–2109, 2007.

[32] D. L. Lombardozzi, M. J. B. Zeppel, R. A. Fisher, and A. Tawfik. Representing nighttime and minimum conductance in CLM4.5: global hydrology and carbon sensitivity analysis using observational constraints. *Geoscientific Model Development*, 10(1):321–331, 2017.

[33] J. Males and H. Griffiths. Economic and hydraulic divergences underpin ecological differentiation in the bromeliaceae. *Plant, Cell & Environment*, 41(1):64–78, 2018.

[34] Y. Malhi, C. Doughty, and D. Galbraith. The allocation of ecosystem net primary productivity in tropical forests. *Philosophical Transactions of the Royal Society B: Biological Sciences*, 366(1582):3225–3245, 2011.

[35] C. Manes, M. Guala, H. Löwe, S. Bartlett, L. Egli, and M. Lehning. Statistical properties of fresh snow roughness. *Water Resources Research*, 44(11), 2008.

[36] W. J. Massman. Water storage on forest foliage: a general model. *Water Resources Research*, 16(1):210–216, 1980.

[37] B. E. Medlyn, R. A. Duursma, D. Eamus, D. S. Ellsworth, I. C. Prentice, C. V. Barton, K. Y. Crous, P. De Angelis, M. Freeman, and L. Wingate. Reconciling the optimal and empirical approaches to modelling stomatal conductance. *Global Change Biology*, 17(6):2134–2144, 2011.

[38] K. Mokany, R. J. Raison, and A. S. Prokushkin. Critical analysis of root: shoot ratios in terrestrial biomes. *Global Change Biology*, 12(1):84–96, 2006.

[39] G.-Y. Niu, Z.-L. Yang, R. E. Dickinson, and L. E. Gulden. A simple TOPMODEL-based runoff parameterization (SIMTOP) for use in global climate models. *Journal of Geophysical Research: Atmospheres*, 110(D21), 2005.

[40] G.-Y. Niu, Z.-L. Yang, R. E. Dickinson, L. E. Gulden, and H. Su. Development of a simple groundwater model for use in climate models and evaluation with gravity recovery and climate experiment data. *Journal of Geophysical Research: Atmospheres*, 112(D7), 2007.

[41] J. Noilhan and S. Planton. A simple parameterization of land surface processes for meteorological models. *Monthly Weather Review*, 117(3):536–549, 1989.

[42] D. F. Parkhurst, P. R. Duncan, D. M. Gates, and F. Kreith. Wind-tunnel modelling of convection of heat between air and broad leaves of plants. *Agricultural Meteorology*, 5(1):33–47, 1968.

[43] J. W. Pomeroy, D. M. Gray, K. R. Shook, B. Toth, R. L. H. Essery, A. Pietroniro, and N. Hedstrom. An evaluation of snow accumulation and ablation processes for land surface modelling. *Hydrological Processes*, 12(15):2339–2367, 1998.

[44] I. C. Prentice, T. Meng, H. Wang, S. P. Harrison, J. Ni, and G. Wang. Evidence of a universal scaling relationship for leaf CO_2 drawdown along an aridity gradient. *New Phytologist*, 190(1):169–180, 2011.

[45] M. R. Raupach. Simplified expressions for vegetation roughness length and zero-plane displacement as functions of canopy height and area index. *Boundary-Layer Meteorology*, 71(1):211–216, 1994.

[46] A. J. Rutter, K. A. Kershaw, P. C. Robins, and A. J. Morton. A predictive model of rainfall interception in forests, I. Derivation of the model from observations in a plantation of Corsican pine. *Agricultural Meteorology*, 9:367–384, 1971.

[47] A. J. Rutter and A. J. Morton. A predictive model of rainfall interception in forests. III. Sensitivity of the model to stand parameters and meteorological variables. *Journal of Applied Ecology*, pages 567–588, 1977.

[48] A. J. Rutter, A. J. Morton, and P. C. Robins. A predictive model of rainfall interception in forests. II. Generalization of the model and comparison with observations in some coniferous and hardwood stands. *Journal of Applied Ecology*, pages 367–380, 1975.

[49] K. Sakaguchi and X. Zeng. Effects of soil wetness, plant litter, and under-canopy atmospheric stability on ground evaporation in the Community Land Model (CLM3.5). *Journal of Geophysical Research: Atmospheres*, 114(D1), 2009.

[50] Y. Sato, T. Kumagai, A. Kume, K. Otsuki, and S. Ogawa. Experimental analysis of moisture dynamics of litter layers - the effects of rainfall conditions and leaf shapes. *Hydrological Processes*, 18(16):3007–3018, 2004.

[51] J. R. Seemann, M. R. Badger, and J. A. Berry. Variations in the specific activity of ribulose-1, 5-bisphosphate carboxylase between species utilizing differing photosynthetic pathways. *Plant Physiology*, 74(4):791–794, 1984.

[52] P. J. Sellers, D. A. Randall, G. J. Collatz, J. A. Berry, C. B. Field, D. A. Dazlich, C. Zhang, G. D. Collelo, and L. Bounoua. A revised land surface parameterization (SiB2) for atmospheric GCMs. Part I: Model formulation. *Journal of Climate*, 9(4):676–705, 1996.

[53] R. H. Shaw and A. R. Pereira. Aerodynamic roughness of a plant canopy: a numerical experiment. *Agricultural Meteorology*, 26(1):51–65, 1982.

[54] K. M. Smits, V. V. Ngo, A. Cihan, T. Sakaki, and T. H. Illangasekare. An evaluation of models of bare soil evaporation formulated with different land surface boundary conditions and assumptions. *Water Resources Research*, 48(12), 2012.

[55] J. S. Sperry, F. R. Adler, G. S. Campbell, and J. P. Comstock. Limitation of plant water use by rhizosphere and xylem conductance: results from a model. *Plant, Cell & Environment*, 21(4):347–359, 1998.

[56] J. S. Sperry and D. M. Love. What plant hydraulics can tell us about responses to climate-change droughts. *New Phytologist*, 207(1):14–27, 2015.

[57] P. Storck, D. P. Lettenmaier, and S. M. Bolton. Measurement of snow interception and canopy effects on snow accumulation and melt in a mountainous maritime climate, Oregon, United States. *Water Resources Research*, 38(11):5–1, 2002.

[58] S. C. Swenson and D. M. Lawrence. A new fractional snow-covered area parameterization for the community land model and its effect on the surface energy balance. *Journal of Geophysical Research: Atmospheres*, 117(D21), 2012.

[59] S. C. Swenson and D. M. Lawrence. Assessing a dry surface layer-based soil resistance parameterization for the Community Land Model using GRACE and FLUXNET-MTE data. *Journal of Geophysical Research: Atmospheres*, 119(17):10–299, 2014.

[60] P. E. Thornton and N. E. Zimmermann. An improved canopy integration scheme for a land surface model with prognostic canopy structure. *Journal of Climate*, 20(15):3902–3923, 2007.

[61] A. A. van de Griend and M. Owe. Bare soil surface resistance to evaporation by vapor diffusion under semiarid conditions. *Water Resources Research*, 30(2):181–188, 1994.

[62] M. A. White, P. E. Thornton, S. W. Running, and R. R. Nemani. Parameterization and Sensitivity Analysis of the BIOME-BGC Terrestrial Ecosystem Model: Net Primary Production Controls. *Earth Interactions*, 4(3):1–85, 2000.

[63] M. Williams, E. B. Rastetter, D. N. Fernandes, M. L. Goulden, S. C. Wofsy, G. R. Shaver, J. M. Melillo, J. W. Munger, S.-M. Fan, and K. J. Nadelhoffer. Modelling the soil-plant-atmosphere continuum in a Quercus–Acer stand at Harvard Forest: the regulation of stomatal conductance by light, nitrogen and soil/plant hydraulic properties. *Plant, Cell & Environment*, 19(8):911–927, 1996.

[64] I. E. Woodrow and J. A. Berry. Enzymatic regulation of photosynthetic CO_2 fixation in C3 plants. *Annual Review of Plant Physiology and Plant Molecular Biology*, 39(1):533–594, 1988.

[65] H.-H. Yeoh, M. R. Badger, and L. Watson. Variations in kinetic properties of ribulose-1, 5-bisphosphate carboxylases among plants. *Plant Physiology*, 67(6):1151–1155, 1981.

[66] X. Zeng, M. Barlage, R. E. Dickinson, Y. Dai, G. Wang, and K. Oleson. Treatment of under-canopy turbulence in land models. *Journal of Climate*, 18(23):5086–5094, 2005.

[67] X. Zeng and R. E. Dickinson. Effect of surface sublayer on surface skin temperature and fluxes. *Journal of Climate*, 11(4):537–550, 1998.

[68] X. Zeng and A. Wang. Consistent parameterization of roughness length and displacement height for sparse and dense canopies in land models. *Journal of Hydrometeorology*, 8(4):730–737, 2007.